FRA-75-5

REPORT NO. FRA-OR&D-75-56

PRELIMINARY ANALYSIS OF THE EFFECTS OF NON-LINEAR CREEP AND FLANGE CONTACT FORCES ON TRUCK PERFORMANCE IN CURVES

A.B. Perlman
H. Weinstock

MAY 1975
INTERIM REPORT

Prepared for
U.S. DEPARTMENT OF TRANSPORTATION
FEDERAL RAILROAD ADMINISTRATION
Office of Reasearch and Development
Washington DC 20590

Technical Report Documentation Page

1. Report No.	2. Government Accession No.	3. Recipient's Catalog No.
FRA-OR&D-75-56		

4. Title and Subtitle	5. Report Date
PRELIMINARY ANALYSIS OF THE EFFECTS OF NON-LINEAR CREEP AND FLANGE CONTACT FORCES ON TRUCK PERFORMANCE IN CURVES	May 1975
	6. Performing Organization Code
7. Author(s) A.B. Perlman, H. Weinstock	8. Performing Organization Report No. DOT-TSC-FRA-75-5
9. Performing Organization Name and Address U.S. Department of Transportation Transportation Systems Center Kendall Square Cambridge MA 02142	10. Work Unit No. (TRAIS) RR515/R5301
	11. Contract or Grant No.
	13. Type of Report and Period Covered Interim Report July 1974-January 1975
12. Sponsoring Agency Name and Address U.S. Department of Transportation Federal Railroad Administration Office of Research and Development Washington DC 20590	14. Sponsoring Agency Code

15. Supplementary Notes

16. Abstract

Prediction of wheel displacements and wheel-rail forces is a prerequisite to the evaluation of the curving performance of rail vehicles. This information provides part of the basis for the rational design of wheels and suspension components, for establishing criteria for maintenance of track and wheels, for use as a guideline for safety standards, and for understanding the mechanism of noise generation and wheel-climbing. The analysis presented here extends the results from linear steady-curving appropriate to flangeless guidance, and provides a foundation for the examination of the details of forces and displacements under more severe conditions necessary to the understanding, prevention, and suppression of undesirable effects.

17. Key Words	18. Distribution Statement
Rail Vehicle Dynamics, Curve Negotiation Mechanics	DOCUMENT IS AVAILABLE TO THE PUBLIC THROUGH THE NATIONAL TECHNICAL INFORMATION SERVICE, SPRINGFIELD, VIRGINIA 22161

19. Security Classif. (of this report)	20. Security Classif. (of this page)	21. No. of Pages	22. Price
Unclassified	Unclassified	44	

Form DOT F 1700.7 (8-72) Reproduction of completed page authorized

PREFACE

The Federal Railroad Administration (FRA) is sponsoring research development, and demonstration programs to provide improved safety, performance, speed, reliability, and maintainability of rail transportation systems at reduced life-cycle costs. A major portion of these efforts is related to improvement of the dynamic characteristics of rail vehicles, track structures.

Under the RR 515 Project, the Transportation Systems Center (TSC) is maintaining a center for resources to be applied to these programs. As part of this effort, TSC has been acquiring, developing, and extending analysis tools to support these FRA objectives.

As a result of a survey of FRA requirements and existing analysis tools, it was found that there is a need for an analytical method of predicting the performance of rail vehicles on curved track taking into account the non-linearities associated with creep forces and the mechanism of flange contact. This report provides a description of in-house efforts to provide a baseline analysis of an idealized truck to provide first-order estimates of the effects of these non-linearities. A more complete model, including a more complete description of rail profile and vehicle/truck non-linearities, is currently under development by Law and Cooperrider under contract DOT-TSC-902 to Clemson University. The major portion of the work described here was performed by Professor A. B. Perlman of Tufts University while under a temporary appointment to the TSC staff.

TABLE OF CONTENTS

LIST OF ILLUSTRATIONS

NOMENCLATURE

A,B,C,D	=	Location of points on the wheel profile
f	=	creep coefficient (force)
f_{xji}	=	longitudinal component of creep force
f_{yji}	=	lateral component of creep force
F_{ji}	=	resultant creep force
F_g	=	gravitational force
$2h\ell$	=	truck wheelbase
h_z	=	change in height of axle load because of lateral displacement
k_L	=	lateral stiffness of wheelset relative to the vehicle body (force per unit displacement)
k_R	=	yaw stiffness of wheelset relative to the vehicle body (couple per unit angle)
2ℓ	=	distance between wheel rail contact points
M_g	=	gravitational moment (couple)
N_{ji}	=	normal force on a wheel
P	=	lateral suspension force on truck
r	=	wheel radius
r_{ji}	=	rolling radius
R	=	curve radius
s	=	distance along track centerline
v_{xji}	=	longitudinal creep velocity
v_{yi}	=	lateral creep velocity
v_{ji}	=	resultant creep velocity
V	=	truck velocity
W	=	wheel load

NOMENCLATURE (CONT'D)

y_i = lateral displacement of wheelset from truck centerline

y_3 = lateral displacement of truck center of gravity

α = wheel profile conicity

α_e = effective conicity

δ_0 = reference point on wheel rail profile

μ = friction coefficient

ϕ_{ji} = angle of wheel contact plane with horizontal

Ψ_2 = wheelset yaw displacement

Ψ_3 yaw displacement of truck body

i = 1, front axle

i = 2, rear axle

j = 1, outside wheel

j = 2, inside wheel

' = derivative with respect to lateral displacement

· = derivative with respect to time.

1. INTRODUCTION

A significant portion of railway track is curved. Negotiation of these curves by freight and passenger vehicles presents problems of wheel and rail wear, noise, and possible derailment which are more severe than for tangent track. The causes of these conditions are generally attributed to large lateral forces resulting from contact of wheel flanges with the rail.

Current attempts to provide improved curving performance include reduction of rotational stiffness of the truck for yaw motion of the axles. Lubrication of center plates, large clearances of components, and parallelogramming of freight trucks and flexible passenger trucks. In combination with large wheel-profile conicity, guidance through curves without flange contact is possible. Recent linear analyses of the dynamics of flexible trucks [1,2,3] have examined the feasibility of steering through the action of creep forces alone. Unfortunately, the requirements of low yaw stiffness and high conicity for flangeless guidance compromise the lateral dynamic stability (hunting characteristics) of rail vehicles on tangent track. For existing designs, curve guidance is produced by a combination of creep force and flange mechanism. The flange mechanism is the dominant means for guidance in tight curves such as those which commonly exist in urban transit properties.

Under these conditions, both creep forces and the gravitational action of the flange are non-linear in nature. The objective of this analysis is to examine the non-linear effects of wheel geometry and creep characteristics over a range of lateral displacements sufficiently large to produce gross sliding motions.

The model for this motion is a flexible truck moving slowly on a curved track. Since the curving performance of a complete vehicle is worse than a single truck, the truck is a first limit for such performance. This baseline model represents the simplest credible account of the non-linearities which provide guidance in the range of lateral displacements on the order of nominal flange

clearance. As such it is employed to obtain bounding condition and qualitative characteristics of the effects of non-linearities on the guidance of vehicles in curves.

2. BACKGROUND

Recent investigations of the dynamics of rail vehicles on curved track have considered the steady motion of a flexible vehicle.[1,2,3] Using linear representations of wheel-profile conicity and creep forces, these analyses have established limits for the minimum curve radius which can be negotiated without slip as a function of the lateral suspension parameters of the vehicle. These results also indicate that the respective outward and inward displacements of the leading and trailing axles of a truck from the rolling position of a free wheelset is strongly influenced by yaw stiffness. On most curves, the linear analysis indicates that stiff trucks either slip or exceed nominal flange clearances. As a result of these conclusions, previous examinations of truck-curving have assumed that trucks were rigid.[4,5,6] In these earlier analyses it is assumed that steering is achieved through friction forces resulting from gross slipping of wheel flanges on rail.

In the construction of new high-speed rail vehicles, the linear, steady-curving analysis has been a basis for rational design of suspension components.[7] However, the design demands for guidance by creep forces only require large flange clearance. In addition, non-linear guidance effects were observed in actual vehicle performance.

As noted elsewhere,[1] the effects of gravity forces on the linear analysis are small as long as the wheel-rail contact is on the wheel tread. As the contact point moves to the root of the flange or to the flange wall, the magnitude of gravity forces become comparable to that of creep. For sufficiently large lateral displacements of the wheels, the creep limit is reached, slip occurs, and the motion is controlled by gravitational effects. In fact, the lateral forces associated with resistance to raising the wheel upon the rail are the essence of the character of the flange.

The analysis presented here extends the work of the linear creep, linear conicity investigations to include regions where

both effects are non-linear. Under some of the conditions where the linear analysis predicts slip steering may in fact be achieved without gross-sliding. However, since inertia effects are neglected, curve entry transients may be somewhat underestimated.

The model, shown in figure 1, is a two-axle, flexible vehicle with profiled wheels traversing a curve of radius, R at a constant forward speed, V. It is described in terms of lateral and yaw displacements of the two wheelsets and the body or frame of the vehicle. The lateral displacements are measured in the direction of the local curve radius and the yaw is referenced to the same radial direction. Wheel gauge (between the contact points with the rail) is denoted by 2ℓ and the vehicle wheelbase by $2\,h\ell$. The flexibility of the suspension is represented by a yaw stiffness, k_R, which resists relative rotation of the axles and the body and lateral stiffness, k_L, which resists relative motion of the ends of the body and the axle centers of gravity.

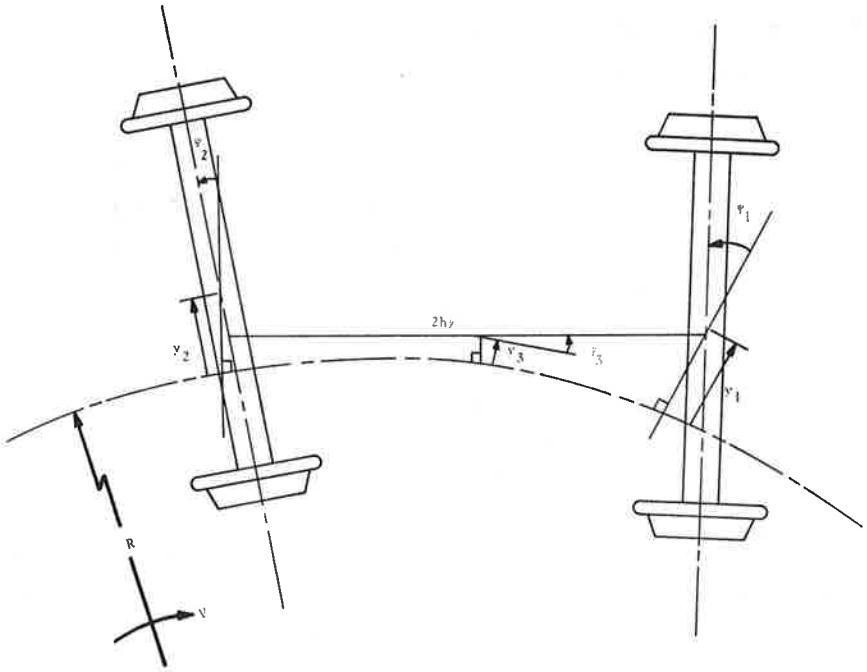

Figure 1. Two-Axle Vehicle Model

3. NON-LINEAR GRAVITATION FORCES

For small lateral displacements of a wheelset, with profiled wheels, the concept of gravitational stiffness has been introduced [8] to represent the lateral forces which resist the movement as a linear function of the lateral displacement. In general however, these forces are non-linearly dependent on the lateral movement of the wheelset. An idealized description of this non-linearity is the knife-edge rail model of figure 2.[9] The gravity effects can be viewed as the lateral force, F_g, required to raise the load on the axle of the wheelset as it is moved over a frictionless rail. Assuming that the yaw of the axle is small and ignoring the compliance of the track, the wheelset will roll through an angle θ as it is displaced a distance, y, laterally. As a result, the potential energy of the axle load, 2W, will be $2Wh_z$, where

$$h_z = y\theta + \left(\frac{r_2 + r_1}{2} - r\right), \tag{1}$$

$$\theta = \frac{r_1 - r_2}{2\ell} \quad . \tag{2}$$

From the Principle of Virtual Work, the work done by the force, F_g, through a virtual displacement, y, is equal to the change of potential energy of the system, so that

$$F_g = \frac{(\text{Potential Energy})}{\partial y} = W\left[\left(\frac{r_1 - r_2}{\ell}\right) + y\left(\frac{r_1' - r_2'}{\ell}\right) + (r_1' + r_2')\right]. \tag{3}$$

For profiled wheels, the rolling radii at the outside and inside contact points of the wheels with the rails are

$$r_1 = r + g\,(y + \delta_0) - g\,(\delta_0), \tag{4a}$$

$$r_2 = r + g\,(\delta_0 - y) - g\,(\delta_0), \tag{4b}$$

where δ_0 is defined by the wheel and track gauges and the wheel rail profiles.

As the wheelset is displaced laterally, the normal forces also produce a torque which tends to destabilize yaw motion and is given approximately as

$$M_g = W \left[g'\,(y + \delta_0) - g'\,(\delta_0 - y) \right] \ell\Psi. \tag{5}$$

In the examples considered here, g(y) will be taken as a polynomial in y representing the wheel profile and g' (y) as the wheel rail contact angle. More generally, g(y) can be viewed as a description of the rolling radius (e.g., experimental determination) as a function of the lateral displacement which accounts for movement of the contact point along the rail head.

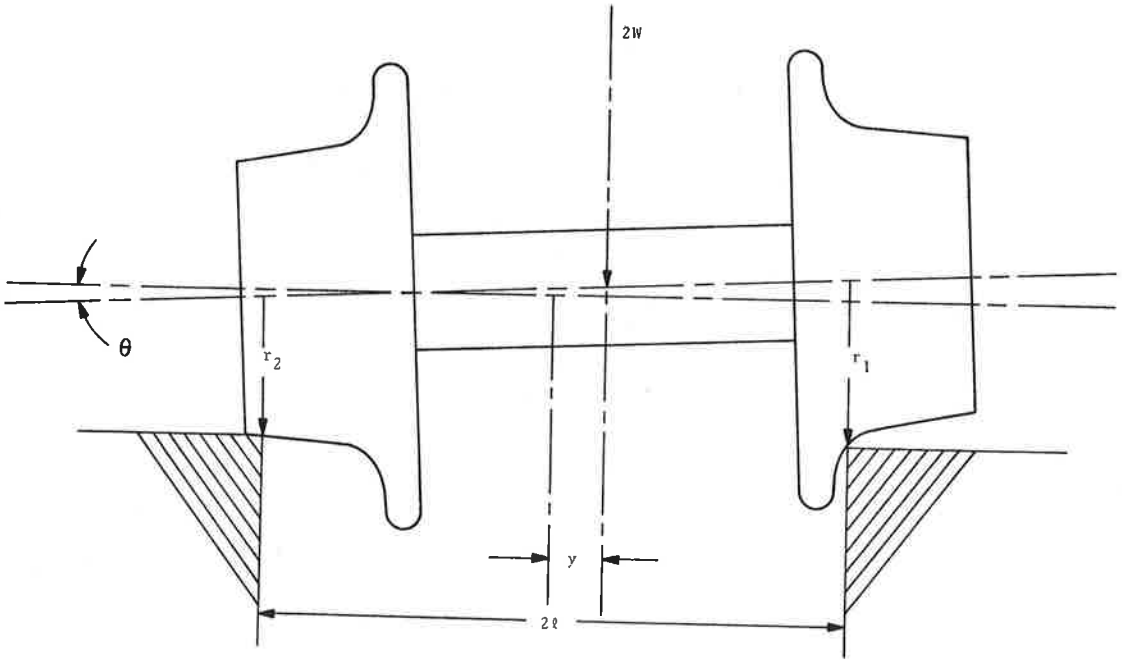

Figure 2. Wheelset with Non-Linear Profile and Knife-Edge Track Representation

4. CREEP FORCES

When the lateral and yaw displacements of a wheel differ from rates consistent with pure rolling motion, creep forces are generated as a result of the relative rates of strain in the contact zone between the wheel and rail. This phenomenon can be described as a functional relationship between the creep forces and difference in actual rolling velocities normalized on the forward speed. Newland[1] has described the details of the appropriate kinematics of a wheelset moving at constant velocity on a turn. In terms of the notation and sign conventions of figure 3, the lateral and longitudinal components of creep velocity for the i^{th} wheelset are

$$v_{yi} = \frac{\dot{y}_i}{V} - \psi_i, \tag{6a}$$

$$v_{x1i} = \frac{r_{1i} - r}{r} + \frac{\ell\dot{\psi}_i}{V} - \frac{\ell}{R}, \tag{6b}$$

$$v_{x2i} = \frac{r - r_{2i}}{r} + \frac{\ell\dot{\psi}_i}{V} - \frac{\ell}{R}. \tag{6c}$$

Ignoring the effect of spin creep, the resultant creep force at each wheel, ${}_jF_{gi}$, is non-linearly related to the resultant creep velocity, v_{ji}, at the corresponding wheel.

$$v_{ji} = \sqrt{v_{yi}^2 + v_{xji}^2}. \tag{7}$$

For large creep velocities, Cooperrider[10] has applied the non-linear functional form of creep curve shown in figure 4 to the analysis of truck-hunting. Assuming, as a first approximation, that the creep coefficients for pure lateral and pure longitudinal

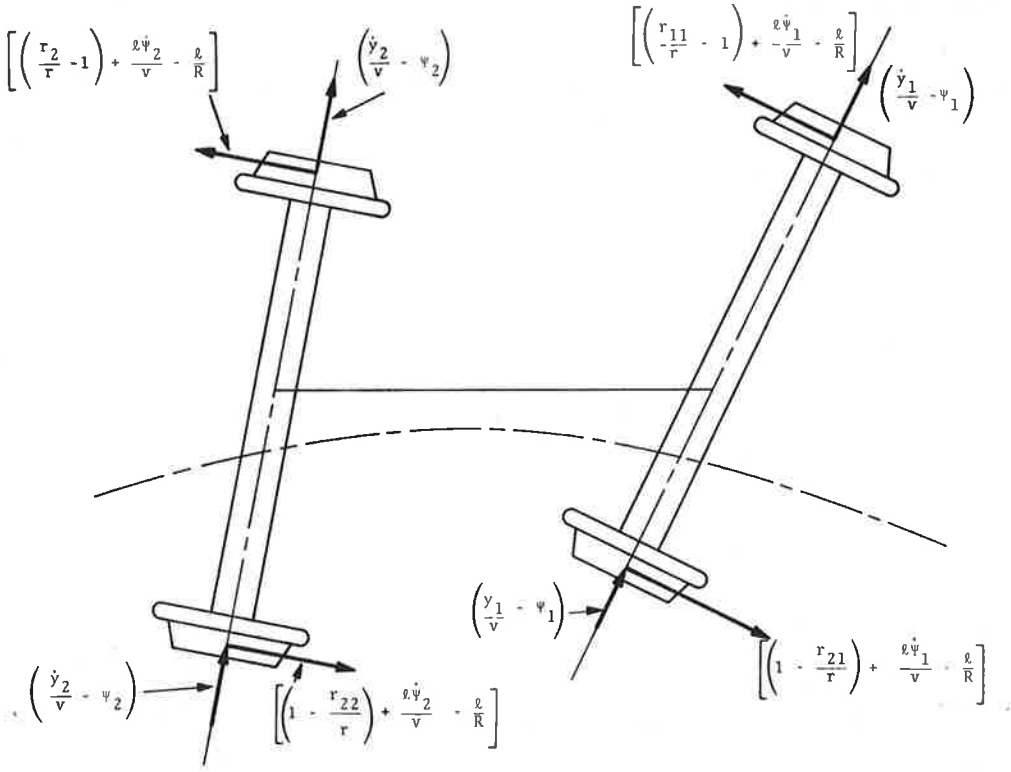

Figure 3. Creep Velocity Components for Two-Axle Vehicle

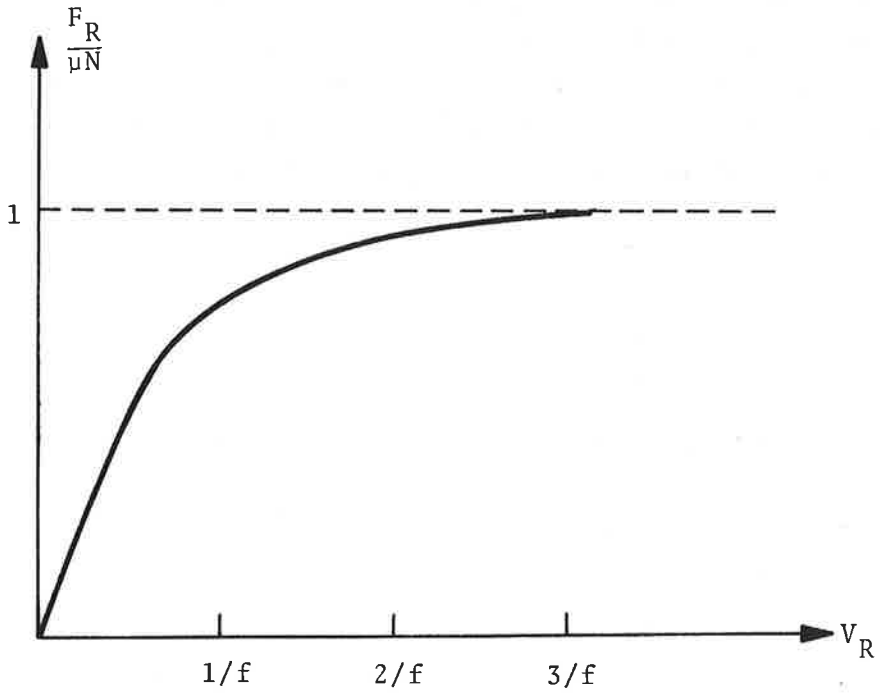

Figure 4. Non-Linear Creep Force Relationship

motion are equal, this creep relation can be expressed as

$$\frac{F_{ji}}{\mu N_{ji}} = f\, v_{ji} - \frac{i}{3}(f\, v_{ji})^2 + \frac{1}{27}(f\, v_{ji})^3; \text{ for } v_{ji} < \frac{3}{f},$$

$$\frac{F_{ji}}{\mu N_{ji}} = 1; \text{ for } v_{ji} > \frac{3}{f}. \qquad (8)$$

Where f, the creep coefficient, is a function of the material and geometry of the contact area, μ is the limiting adhesion or friction coefficient, and N_{ji} the normal force between the wheel and rail. When the contact point is on the flange wall, N_{ji} is taken such that its vertical component equals the wheel load; i.e.,

$$N_{ji} \cos \phi_{ji} = W, \qquad (9)$$

$$\phi_{ji} = \tan^{-1} r'_{ji}. \qquad (10)$$

The resultant creep force can be resolved into lateral and longitudinal components which act to oppose the motion of their corresponding creep velocities. These components of creep force are as follows:

$$f_{yji} = v_{yi}\, f_{ji}, \qquad (11a)$$

$$f_{xji} = v_{xji}\, f_{ji}. \qquad (11b)$$

Where f_{ji} is the effective creep coefficient of wheel j as defined by

$$f_{ji} = \frac{F_{ji}}{v_{ji}}. \qquad (12)$$

The effect of these creep forces on each wheelset is a lateral force,

$$F_{ci} = f_{y1i} + f_{y2i}, \tag{13}$$

and a yaw couple,

$$M_{ci} = \ell(f_{x1i} + f_{x2i}), \tag{14}$$

as shown in figure 5.

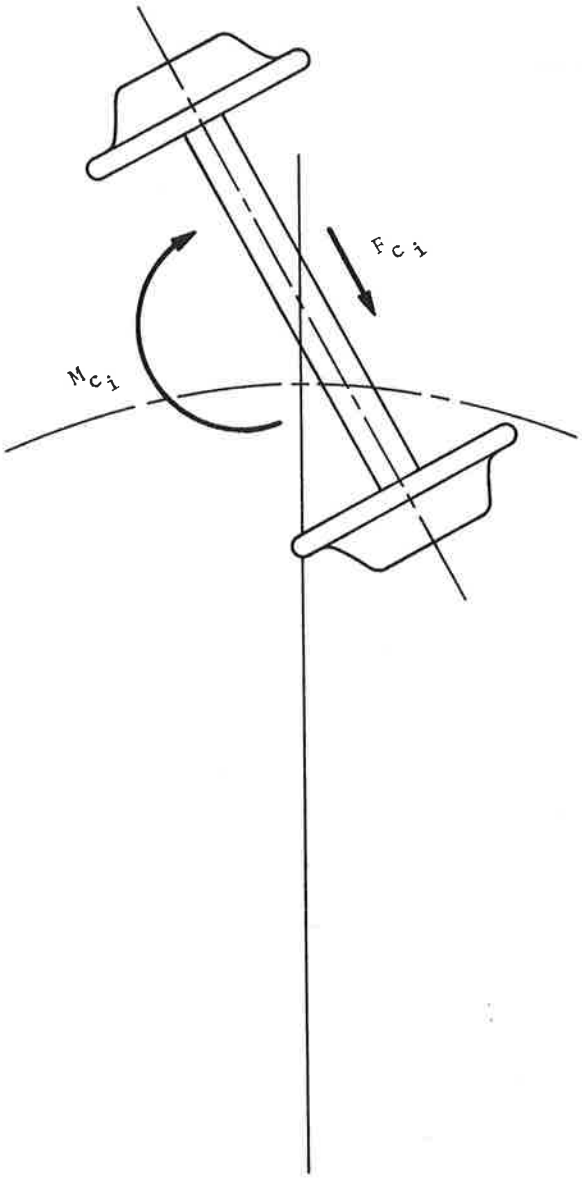

Figure 5. Creep Force and Couple Acting on i^{th} Wheelset

5. EQUATIONS OF MOTION

If the effects of the vehicle and axle inertia for yaw and lateral accelerations are small compared with creep and gravitational forces, the motion of the vehicle will be determined by a balance of the suspension forces against creep and gravitation. Such conditions prevail for steady-curving,[1,2] but are also a reasonable approximation of the motion of a vehicle moving slowly along a curve. In contrast with steady-curving, the rates of yaw and lateral displacement for the latter situation can be non-zero so that creep (and therefore all)forces may vary. As long as no slip occurs, this motion is the kinematic mode for a flexible vehicle on curved track. For a given set of initial conditions, the displacements are a function of the distance traveled along the curve and are independent of the speed of the vehicle. The gravitational effects of a vehicle traveling at a velocity which differs from the balance speed for superelevation of the track can be represented by a lateral force, P, applied to the body of the vehicle.

Consistent with the assumptions of small inertia effects, gyroscopic terms can be ignored. The balance of creep, gravitation, and suspension forces are described by six equations for yaw and lateral equilibrium of the two wheelsets and for the body. Considering equations (13) + (14), these conditions can be written as

$$k_L (y_1 - y_3 - h\ell\psi_3) = -F_{c1} - F_{g1} , \qquad (15a)$$

$$k_L (y_2 - y_3 + h\ell\psi_3) = -F_{c2} - F_{g2} , \qquad (15b)$$

$$k_R (\psi_1 - \psi_3 - \frac{h\ell}{R}) = M_{c1} + M_{g1} , \qquad (15c)$$

$$k_R (\psi_2 - \psi_3 + \frac{h\ell}{R}) = -M_{c2} + M_{g2} , \qquad (15d)$$

$$k_L \quad (2y_3 - y_1 - y_3) = P \quad , \tag{15e}$$

$$k_R \quad (2\Psi_3 - \Psi_1 - \Psi_2) + k_L \, h\ell \, (y_2 - y_1 + 2h\ell\Psi_3) = 0 \tag{15f}$$

By substituting from equations (6) to (14), the equation of motion can be solved in terms of the lateral and yaw displacement rates. Noting that $\frac{ds}{dt} = V$, these rates can be expressed as a function of the distance along the track.

$$\frac{dy_i}{ds} = \Psi_1 - \frac{1}{f_{1i} + f_{2i}} \left[F_{gi} + k_L \, (y_i - y_3 \mp h\ell\Psi_3) \right] , \tag{16a}$$

$$\frac{d\Psi_i}{ds} = \frac{1}{R} - \frac{1}{\ell(f_{1i} + f_{2i})} \left[f_{1i} \left(\frac{r_{1i}}{r} - 1 \right) + f_{2i} \left(1 - \frac{r_{2i}}{r} \right) \right.$$

$$\left. -M_{gi} + k_R \left(\Psi_i - \Psi_3 \mp \frac{h\ell}{R} \right) \right] . \tag{16b}$$

The minus and plus signs correspond to i = 1 (front axle) and i = 2 (rear axle), respectively. The motion of the body is determined by the positions of the wheelsets and the force, P.

$$y_3 = \frac{1}{2} \left[(y_1 + y_2) + \frac{P}{k_L} \right] , \tag{17a}$$

$$\Psi_3 = \frac{1}{2} \left[\frac{k_R \, (\Psi_1 + \Psi_2) + k_L h\ell (y_1 - y_2)}{k_R + (h\ell)^2 \, k_L} \right] . \tag{17b}$$

6. RESULTS

The set of non-linear, first-order differential equations (16) was programmed for numerical integration on a digital computer using a fourth-order Runge-Kutta algorithm. Right-hand sides of the equations were calculated by proceeding from displacements at each wheel sequentially through computation of rolling radii, gravitational forces and couples, normal forces, creep velocities, and creep forces. Reduced step sizes were generally required for conditions of large creep or slip. Typical run times for 40 steps on a DEC 10 computer were on the order of 10 seconds.

6.1 WHEELSET

Motion in the kinematic mode is illustrated by the lateral displacement of an unrestrained wheelset with constant conicity wheels (Fig. 6). Starting from zero initial conditions (i.e., at the track centerline with no yaw), the displacement is a sinusoid with a mean value and an amplitude equal to the steady-curving tracking error, $y_0 = \frac{r\ell}{R\alpha}$, predicted by the linear theory. (Parameters for those examples were selected to facilitate comparison with results of the linear analysis presented elsewhere .[1]) For smaller wheel conicity, α, both the amplitude and wavelength of the displacement increase. This sinusoid about the steady-tracking position is identical to the motion called kinematic-hunting of conical wheels about the centerline of tangent track which has wavelength given by $2\pi \frac{r\ell}{\alpha}$. If the wheelset is started from the conditions for steady-curving, there is no oscillatory motion. In this case, steady motion is essentially pure-rolling. The axle lines up with the local radius so that there is no yaw, and the steady motion requires no longitudinal creep force. Only a very small lateral creep force is needed to offset the gravitational force. For the oscillatory motion, some longitudinal creep force acts to turn the axle. However at displacements consistent with the linear theory, creep forces can be taken as negligible, and a

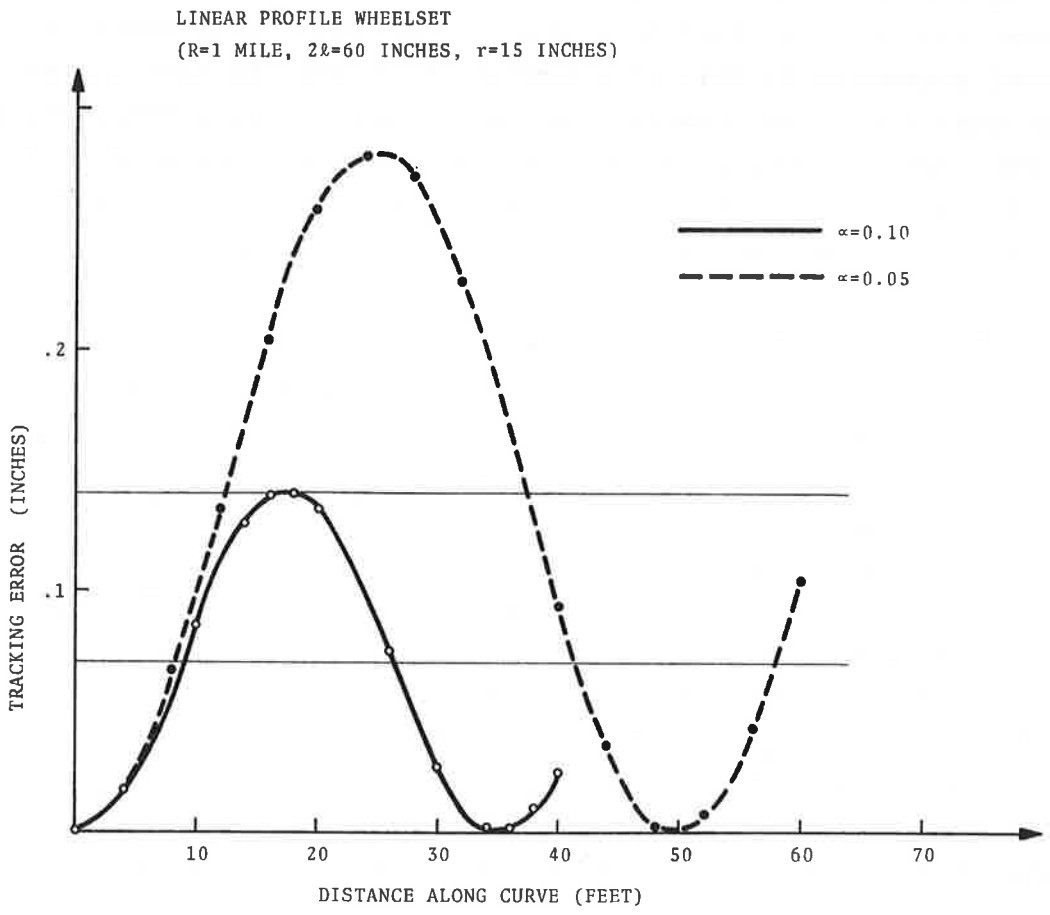

Figure 6. Kinematic Mode of Wheelset with Linear Profile

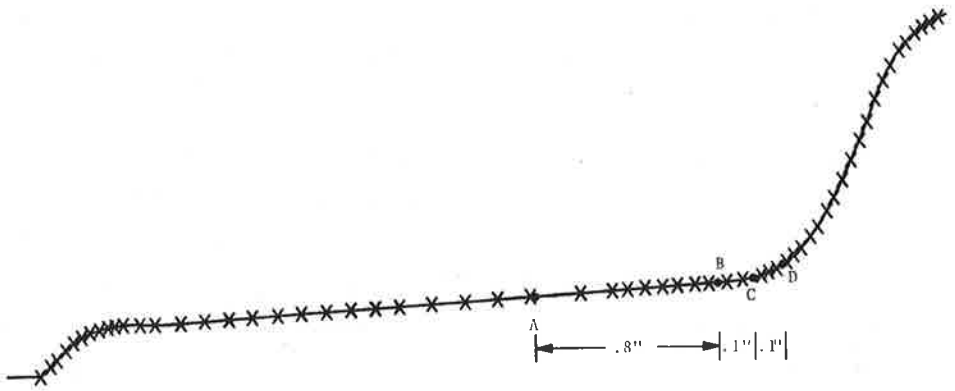

Figure 7. Polynomial Representation of Narrow Flange Profile

free wheelset with a linear profile should negotiate a curve of any radius without slipping.

To investigate the effects on non-linear geometry, the Association of American Railroads'(AAR) standard narrow flange wheel profile was approximated by the high-order polynomial of figure 7. Since this representation does not account for the movement of the wheel-rail contact point along the railhead, a neutral-rolling contact point at a nominal location, A, allows an unreasonably large representation of flange clearance. For the contact point at B, C, or D, the clearance can be presented more realistically as shown in figure 8. The gravitational force computed from equation (3) reaches a maximum roughly when the slope stops increasing about half-way up the flange. The curve corresponding to a neutral point A is essentially that for a constant 1/20-conicity.

Figure 9 represents the lateral motion of the free wheelset with the neutral radius at c on a moderate curve (R = 1 mile). Qualitatively, this motion is similar to that of the linear geometry. The sinusoidal oscillation about the steady-tracking position has an amplitude dependent on the initial conditions. The dotted curve is the lateral displacements started from a position corresponding to the conicity at c. For this geometry, the mean displacement, the steady-tracking error, is reduced to a value, $y_0 = \frac{\ell r}{\alpha_e R}$. α_e is an effective conicity,[2] $\frac{r_1 - r_2}{2y_0}$, for radii r_1 and r_2 computed at the steady-tracking position. Figure 10 illustrates the influence of effective conicity on the predicted steady-tracking position for the standard wide-flange profile. The steady-tracking curve for each contact point was determined by computing the rolling radii and effective conicity for a given lateral displacement, and then, calculating the curve radius consistent with a tracking error equal to the displacement. The limiting effect of the flange is clearly evident in contrast with the linear-profile prediction. One simple interpretation of these curves would be in terms of a nominal flange clearance limit on curve radius. For a nominal clearance of 0.3 inch, the linear-profile limit would be about 2500 feet, while the limit from the curve point "c" is 1300 feet.

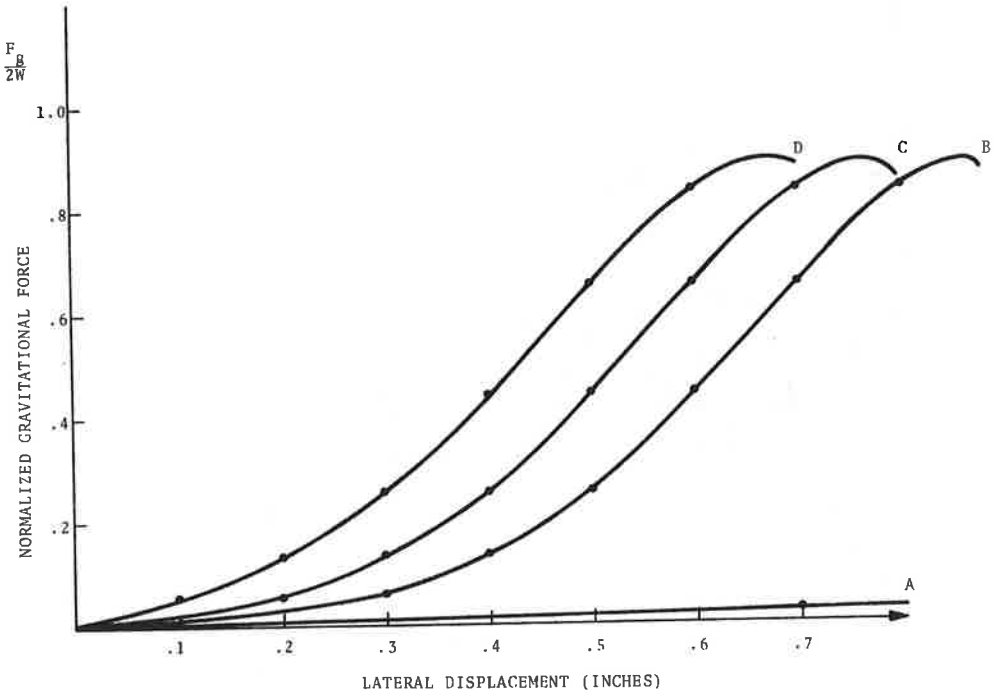

Figure 8. Gravitational Force for Wide Flange Profile

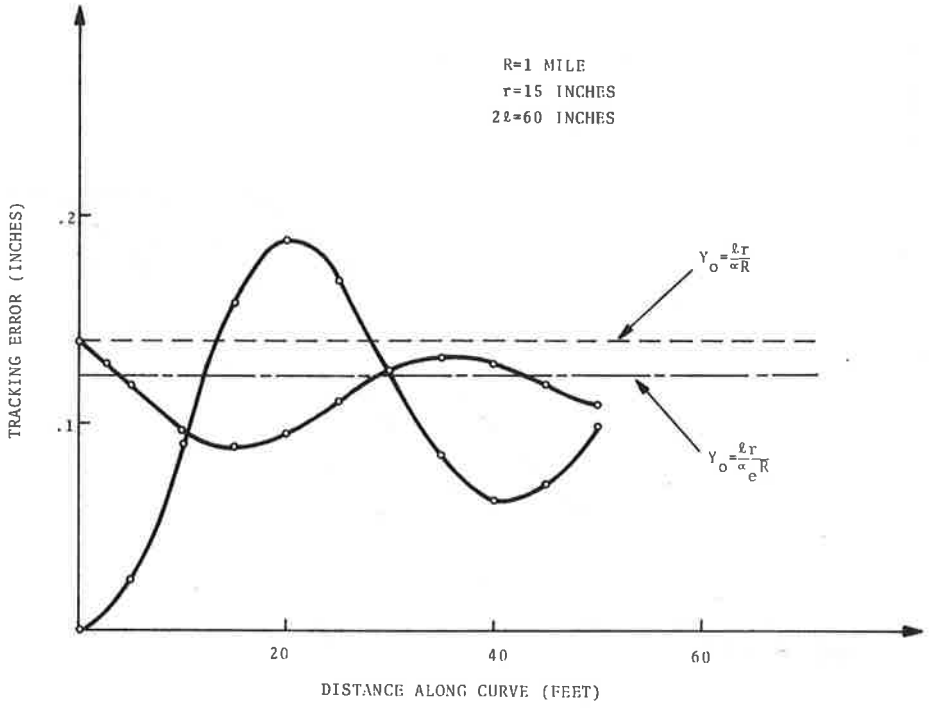

Figure 9. Kinematic Mode of Non-Linear Profile Wheelset with Neutral Radius at Point C

As the radius of the curve becomes smaller, the effect of the geometric non-linearity can interact with the non-linear form of the creep forces. In contrast with the linear theory, the steady-tracking position of the wheelset can be limited by the coefficient of friction rather than by the effective conicity. For example, at R = 500 feet, the y_0 from curve "c" for the sample wheelset is 0.451. As shown in figure 11, for $\mu = 0.2$, the motion of the wheelset is highly damped and quickly reaches steady value of 0.367. This is a sliding rather than a rolling motion.

This steady position in slip motion can be determined by a reasonable approximation from an examination of equations (15). Noting that steady conditions correspond to a lateral displacement for which the algebraic sum of the creep and gravitational forces is zero, y can be computed from the gravitational force required for this balance. In the steady motion, the yaw displacement of the wheelset it negligible. Therefore, the resultant creep force is essentially pure lateral since little longitudinal component is needed to offset the gravitational couple. For a given coefficient of friction, the maximum creep force at each wheel is limited to μN. The F_g required to balance the total lateral creep force on the wheelset is, therefore, approximately $2\mu W$. A graph such as figure 8 can be used to determine the lateral displacement corresponding to that value of F_g. As indicated in figure 11, as μ increases, the wheel can climb farther up the flange. When slipping finally occurs, the displacement adjusts to the steady-tracking position consistent with the effective conicity. These results give an indication of adhesion as an agent providing the mechanism for wheel-climbing which may lead to derailment.

Thus for a given curve radius, the steady-curving position will be the minimum of the limiting friction or the effective conicity value. Alternatively, the limiting friction can be interpreted in terms of the minimum radius for which the wheelset will not slip. As indicated in figure 11 for the profile characterized by the curve "c", this limiting radius is 870 feet for $\mu = 0.2$, and 6.20 feet for $\mu = 0.3$.

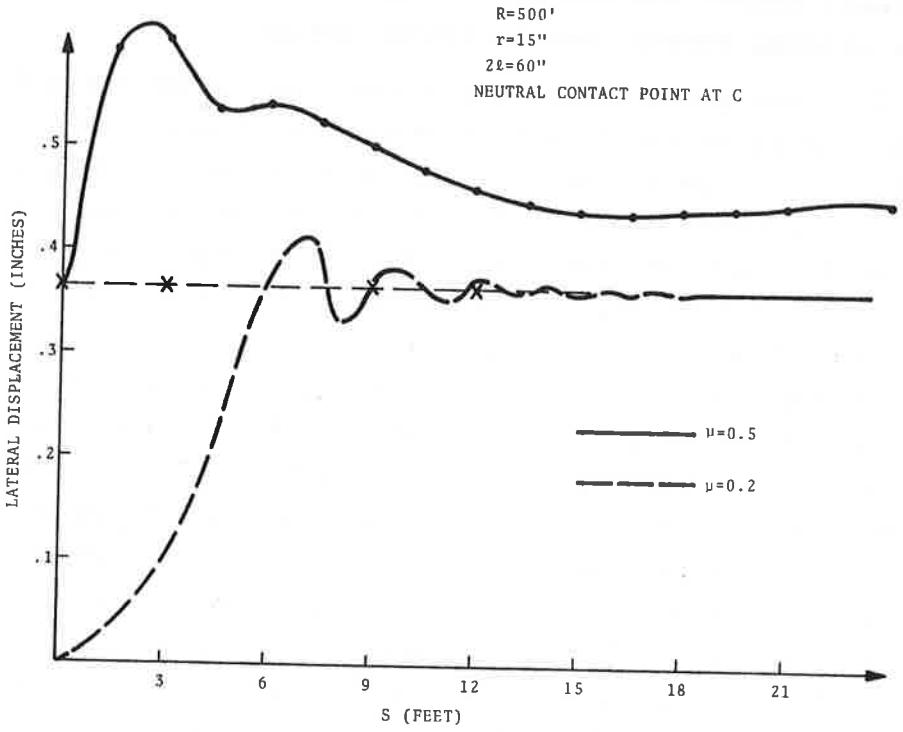

Figure 10. Steady Tracking Position for Non-Linear Profile

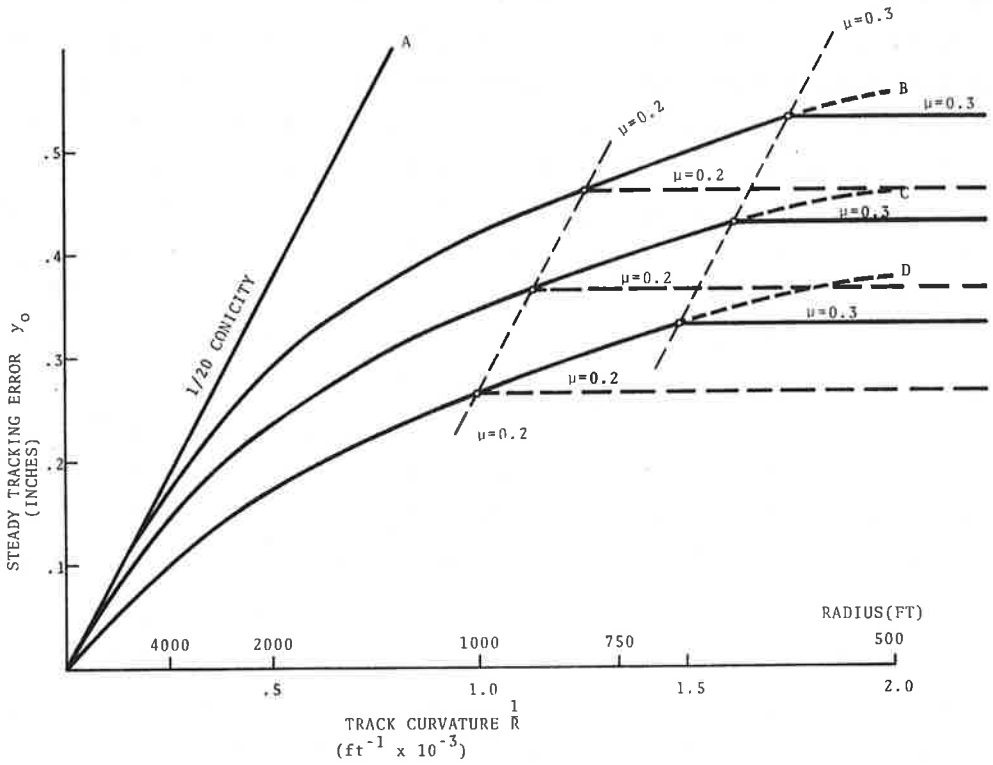

Figure 11. Effect of Friction Coefficient on Non-Linear Wheelset Displacement

6.2 FLEXIBLE VEHICLE

When suspension elements are present in the vehicle which restrain the yaw and lateral motion relative to the body of the vehicle, the kinematic mode of motion differs from that of the free wheelset. Even on curves with a radius large enough that no slipping occurs, creep forces of significant magnitude may be generated to guide the vehicle. A motion typical of a flexible vehicle for such conditions is shown in figure 12. In this example with constant conicity wheels, the characteristic lateral motion of each wheel is a damped sinusoid which is asymptotic to the steady-tracking position predicted by the linear theory. The wavelength and damping ratios of these trajectories are functions of the lateral and yaw stiffness. This motion is analogous to the kinematic mode of a flexible truck on tangent track for which the wavelength and damping vary between the values for a free wheelset and for a rigid truck.[9,11,12] The difference in magnitudes of the motion of the leading and trailing axles is characteristic of the angle of attack with respect to the centerline which the flexible truck adopts since it cannot roll through the curve.

Some of the effects of the creep and geometric non-linearities on this basic kinematic behavior are shown in figure 13. The example truck is moderately flexible with the straightline representing the linear-theory prediction[1] of three times the corresponding displacement of a free wheelset. For a linear profile but non-linear creep, the dotted curve follows the non-linear saturation characteristic of the creep curve. It is asymptotic to a slipping radius limit. This result is consistent with experimental results reported by Boocock[2] for a model vehicle on a roller rig and provides a means for laboratory determination of a limiting friction. The dashed curve represents the combined effects of non-linear creep and non-linear profile (neutral contact point taken at "c" in Fig. 7). As can be seen from the terminations of the plots, the limiting curve radius for no slip is strongly influenced by the non-linearities.

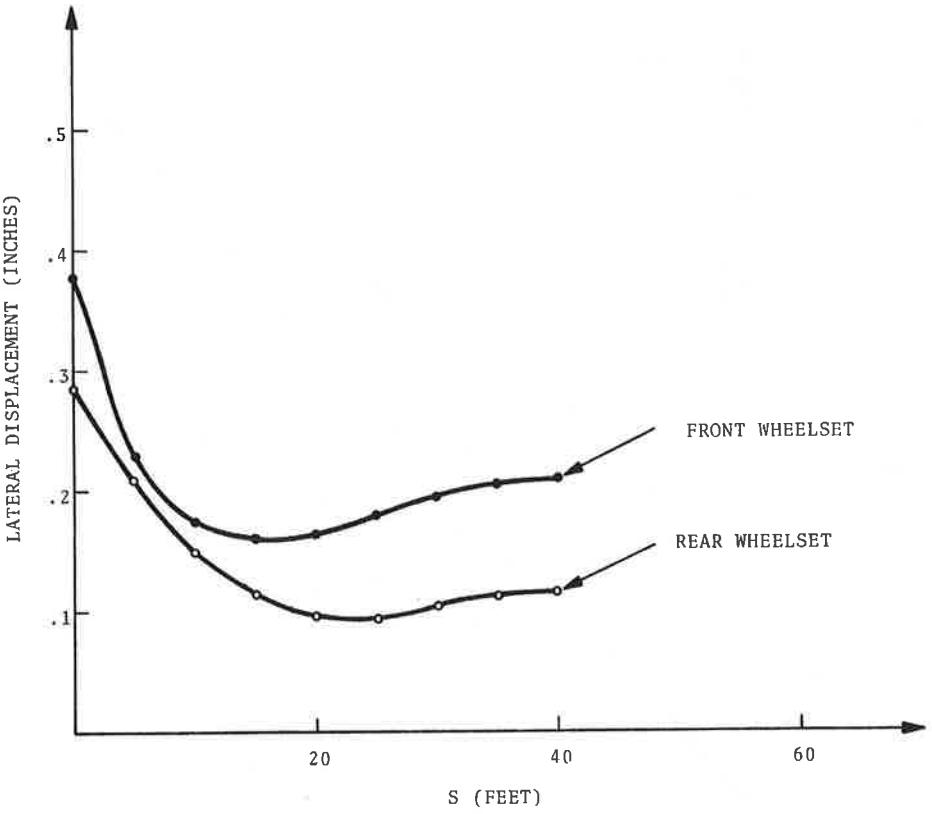

Figure 12. Kinematic Mode of Flexible Truck with Linear Profile Wheels

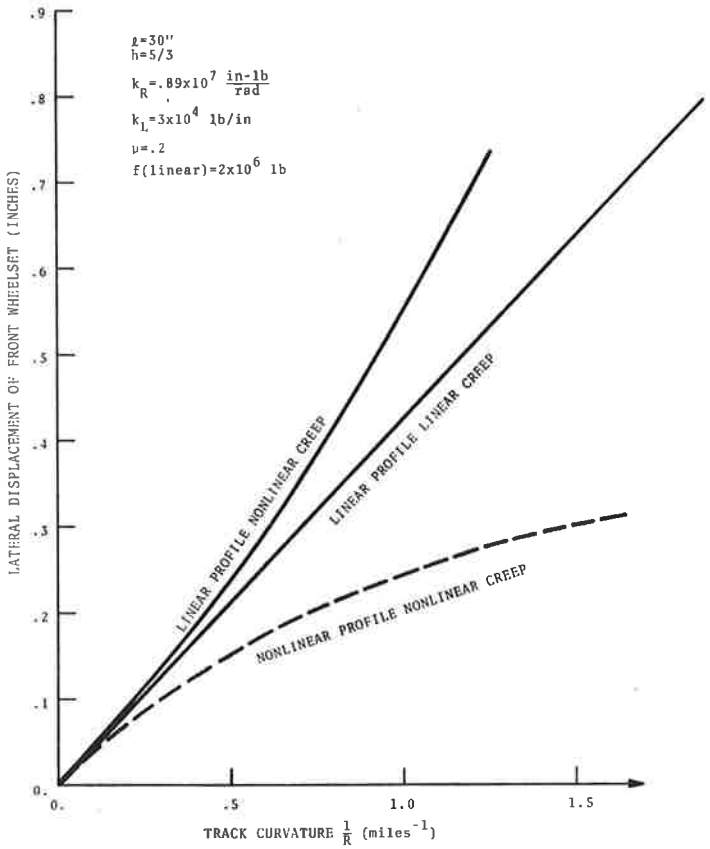

Figure 13. Effect of Non-Linearities on Flexible Truck Displacement

However, with the non-linear results available, a modification of the linear interpretations is possible. For example, Newland[1] has represented the lateral displacements of the wheelsets of the flexible truck as a function of non-dimensional yaw-and-lateral stiffness parameters. The displacements are particularly sensitive to the yaw-stiffness parameter, $K_1 = \frac{k_R}{2fh\ell}$, in which the creep coefficient, f, is taken as the slope of the creep curve for the linear, small creep-velocity range. For relatively high-yaw stiffness, the creep forces required even for steady-curving may be a large fraction of the total available creep. It can be seen from figure 4 that at large creep velocities, the effective creep coefficient is reduced as compared with the linear value of the initial slope. In figure 14, the normalized steady-tracking error of the front wheelset of a flexible vehicle with linear profile wheels (conicity = 0.05), but non-linear creep forces, is compared with results of the linear analysis.[1] The deviation of the linear and non-linear results can be interpreted in terms of the effective creep coefficient, shifting the linear results shown in figure 14 to the left-hand to account for an increase in the dimensionless yaw stiffness (i.e., the lateral displacement corresponds to a yaw-stiffness parameter with f equal to the effective rather than the linear creep coefficient).

A similar interpretation can be associated with the steady-curving results for a vehicle with non-linear creep and non-linear wheel profile. If no slip occurs in the steady-tracking, the lateral displacement can be related to the corresponding tracking error for a free wheelset with the same wheel profile. In this case, the lateral displacements in the non-dimensional tracking error are computed from the effective conicity, while K_1 corresponds to the effective creep coefficient.

In contrast with the free wheelset, significant components of both longitudinal-and-lateral creep force are required to steer a flexible vehicle. The approximation of gravitational force offsetting lateral creep at slip conditions cannot be readily extended for non-linear geometry and creep of the vehicle. However, an effective creep force can be calculated from the resultant creep force computed by the program for steady-curving conditions. This

coefficient can then be used to modify the linear results, such as Newland's non-dimensional curve radius, $R_\mu = W/fh\ell$, to determine a minimum radius for steady-curving without slip. A similar argument can be applied to modify the linear prediction of superelevation effects.

As the results of the free wheelset kinematic motion indicate, the forces and slip conditions in transient motion such as curve entry are likely to be more severe than those of steady-curving. While the design of spiral track sections is intended to alleviate the effects of entry, local disturbances produce motions significantly different from steady-curving. For such circumstances, the linear predictions cannot be readily modified so that force magnitudes and conditions of slip must be determined from exercise of the computer program for specific vehicle and curve geometry, suspension parameters, and initial conditions.

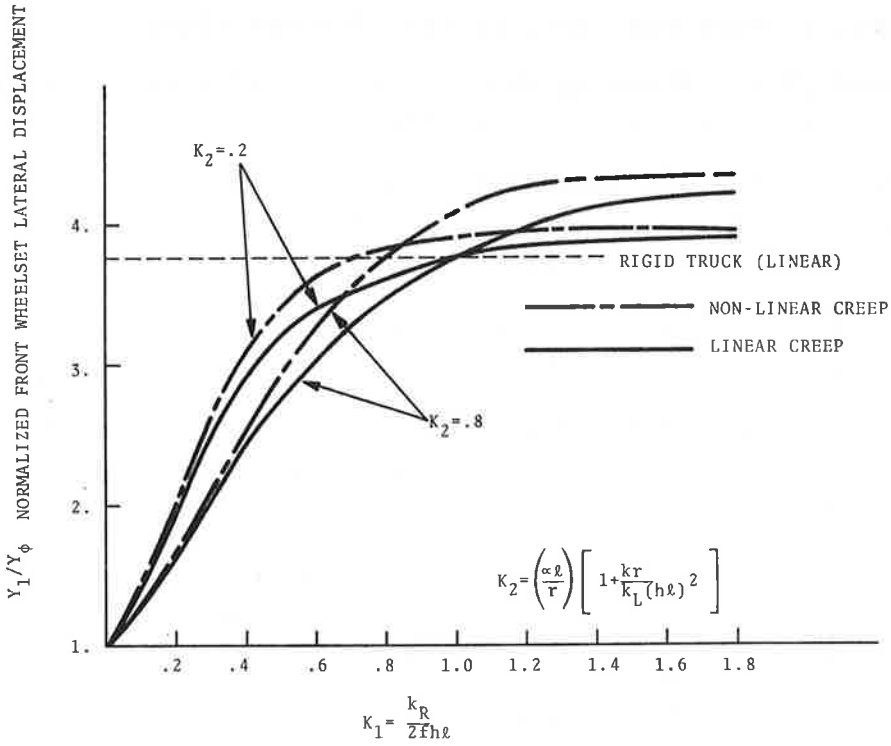

Figure 14. Effect of Non-Linear Creep on Non-Dimensional Wheelset Displacement

7. REFERENCES

1. Newland, D.E., Steering a Flexible Railway Truck on Curved Track, J. Eng. Ind., Trans. ASME, Ser. B, 91 (3), 908-918 (Aug. 1969).

2. Boocock, D., Steady State Motion of Railway Vehicles on Curved Tracks, J. Mech Eng. Sci. 11 (6), 556-566 (1969).

3. Newland, D.E., Steering Characteristics of Bogies, The Railway Gazette, 745-750 (Oct. 4, 1958).

4. Müller, C.Th., Dynamics of Railway Vehicles on Curved Track, Interaction Between Vehicle and Track, Proc. Inst. Mech. Eng. 180 (Pt. 3F), 45-57 (1966).

5. Cain, B.S., Vibration of Rail and Road Vehicles, Pitman, NY NY (1940).

6. Koci, L.F. and Marta, H.A., Lateral Loading Between Locomotive Truck Wheels and Rail due to Curve Negotiation, ASME, Paper No. 65-WA/RR-4 (1965).

7. Hobbs, A.E.W. and Pearce, T.G., The Lateral Dynamics of the Linear Induction Motor Test Vehicle, J. Dyn. Sys.,Meas. Cont., Trans. ASME, Ser. G, 96, (2), 147-157 (June 1974).

8. Wickens, A.H., The Dynamic Stability of Railway Vehicle Wheelsets and Bogies Having Profiled Wheels, Internatl. J. Solids Struct. 1, 319-341 (1965).

9. Weinstock, H., Analysis of Rail Vehicle Dynamics in Support of Development of the Wheel Rail Dynamics Research Facility, Int. Rept., U.S. D.O.T., PB 222654 (June 1973).

10. Cooperrider, N.K., The Hunting Behavior of Conventional Railway Trucks, J. Eng. Ind. Trans. ASME, Ser. B., 94 (2), 752-762 (May 1972).

11. Anon., Wrought Steel Wheels and Forged Railway Axles: Steel Products Manual, Am. Iron Steel Inst. (Sep. 1973).

12. Perlman, A.B., An Experimental Parametric Study of the Effect of Flexibility of the Lateral Dynamics of Rail Vehicle Trucks, On File at TSC, U.S. D.O.T. (Aug. 1972).